promoting access to White Rose research papers

Published paper

Therapeutics

ORIGINAL RESEARCH COMMUNICATION

Ru(CO)$_3$Cl(Glycinate) (CORM-3): A Carbon Monoxide–Releasing Molecule with Broad-Spectrum Antimicrobial and Photosensitive Activities Against Respiration and Cation Transport in *Escherichia coli*

Jayne Louise Wilson,[1] Helen E. Jesse,[1] Bethan Hughes,[1] Victoria Lund,[1] Kathryn Naylor,[1]
Kelly S. Davidge,[1,*] Gregory M. Cook,[2] Brian E. Mann,[3] and Robert K. Poole[1]

Abstract

Aims: Carbon monoxide (CO) delivered to cells and tissues by CO-releasing molecules (CO-RMs) has beneficial and toxic effects not mimicked by CO gas. The metal carbonyl Ru(CO)$_3$Cl(glycinate) (CORM-3) is a novel, potent antimicrobial agent. Here, we established its mode of action. *Results:* CORM-3 inhibits respiration in several bacterial and yeast pathogens. In anoxic *Escherichia coli* suspensions, CORM-3 first stimulates, then inhibits respiration, but much higher concentrations of CORM-3 than of a classic protonophore are required for stimulation. Proton translocation measurements (H$^+$/O quotients, *i.e.*, H$^+$ extrusion on pulsing anaerobic cells with O$_2$) show that respiratory stimulation cannot be attributed to true "uncoupling," that is, dissipation of the protonmotive force, or to direct stimulation of oxidase activity. Our data are consistent with CORM-3 facilitating the electrogenic transmembrane movement of K$^+$ (or Na$^+$), causing a stimulation of respiration and H$^+$ pumping to compensate for the transient drop in membrane potential ($\Delta\Psi$). The effects on respiration are not mimicked by CO gas or control Ru compounds that do not release CO. Inhibition of respiration and loss of bacterial viability elicited by CORM-3 are reversible by white light, unambiguously identifying heme-containing oxidase(s) as target(s). *Innovation:* This is the most complete study to date of the antimicrobial action of a CO-RM. Noteworthy are the demonstration of respiratory stimulation, electrogenic ion transport, and photosensitive activity, establishing terminal oxidases and ion transport as primary targets. *Conclusion:* CORM-3 has multifaceted effects: increased membrane permeability, inhibition of terminal oxidases, and perhaps other unidentified mechanisms underlie its effectiveness in tackling microbial pathogenesis. *Antioxid. Redox Signal.* 19, 497–509.

Introduction

CARBON MONOXIDE (CO) is an environmental pollutant and poison but, in biology and medicine, only the reactions of CO with hemes (3,9) are generally appreciated. However, CO, similar to nitric oxide and hydrogen sulfide, is also a "gasotransmitter" with wide-ranging benefits, including vasodilation, antioxidant effects, and roles in inflamma-

tory signaling (40). Administration of CO to animals exposed to endotoxin decreases inflammation and attenuates injury (3). CO enhances phagocytosis of heat-killed *Escherichia coli* (44) by RAW 264.7 cells, and CO from the CO-releasing molecule-3 [Ru(CO)$_3$Cl(glycinate), CORM-3] decreases *Pseudomonas aeruginosa* counts in the spleen, allowing increased survival in mice following experimental bacteremia (15). Moreover, heme oxygenase (HO)–deficient mice suffer

[1]Department of Molecular Biology and Biotechnology, and [3]Department of Chemistry, The University of Sheffield, Sheffield, United Kingdom.
[2]Department of Microbiology and Immunology, University of Otago, Dunedin, New Zealand.
*Current affiliation: Centre for Biomolecular Sciences, University of Nottingham, Nottingham, United Kingdom.

Innovation

Carbon monoxide–releasing molecules (CO-RMs) are being investigated for potential use in delivering CO to cells and tissues and show promising early results as antimicrobial agents. Since the modes of CO-RM action are probably dissimilar to currently used antibiotics, CO-RMs have the potential for topical or targeted treatment of antibiotic-resistant bacteria. However, rational design and exploitation of CO-RMs requires a fundamental understanding of their activity. We report that $Ru(CO)_3Cl(glycinate)$ has complex, time-dependent effects on bacteria, including stimulation and inhibition of respiration, and promotion of transmembrane cation transport, highlighting the potential of CO-RMs for multifaceted, broad-spectrum utilization in clinical microbiology.

exaggerated lethality from polymicrobial sepsis (7) and targeting HO-1 to blood vessels and bowel ameliorates sepsis-induced death. Importantly, injection of CO-RM into wild-type mice increases phagocytosis of *Enterococcus faecalis* and rescues HO-1-deficient mice with experimental sepsis (7). Thus, CO administration may be a clinically useful intervention in microbial infections (6,40).

Nevertheless, the mode(s) of action of CO and CO-RMs remain unclear. We have shown that CORM-3 enters cells, delivers CO to intracellular oxidases (11), and inhibits bacterial growth. In addition, transcriptome profiling of the response of *E. coli* to CORM-3 reveals downregulated expression of respiratory genes; however, the modularity and redundancy of bacterial respiration (47) suggests that a functioning respiratory system would persist (11), so the impact on respiration remains uncertain. Evidence for previously unrecognized activity of CO in bacteria comes from the transcriptomic effects on genes involved in metal metabolism, homeostasis, and transport (11). Probabilistic modeling (52) of the microarray data identified the involvement of eight transcription factors (11), only two of which (ArcA and FNR) have direct roles in regulation of respiration. In another transcriptomic study, using tricarbonyl dichlororuthenium (II) dimer (CORM-2), respiratory genes were not major targets (42). Intriguingly, although solutions of CO gas also impair bacterial growth (43), they do not match the effectiveness of CORM-2 or CORM-3 (11).

Here, we describe for the first time direct evidence for "classical" inhibition of respiration by any CO-RM. That the action of CO-RM-derived CO is due to binding of CO to hemoproteins is demonstrated by photorelief of respiratory inhibition and bacterial killing. We also demonstrate transient stimulation of respiration similar to the "uncoupler"-like action of CORM-3 on mitochondria recently reported (22). However, we attribute it not to protonophore activity, but to facilitation of cation transport.

Results

CORM-3 both stimulates and inhibits bacterial respiration

CO release from CORM-3, using dithionite-reduced myoglobin as a CO trap, is complete in < 10 min (8,38). However, recent measurements with myoglobin in the absence of dithionite (which greatly enhances CO release) or oxyhemoglobin as a trap for the released CO show that CORM-3 liberated no detectable CO in 1 h (38). A previous study, however, revealed that high CORM-3 concentrations (125–250 μM) dramatically inhibited *E. coli* respiration within 30 min, whereas 30 μM CORM-3 elicited major changes in transcript levels within 15 min (11).

We, therefore, investigated whether CORM-3 inhibits respiration in a timeframe that is consistent with the rapid loss of CO in certain biological experiments. *E. coli* cells were incubated in an O_2 electrode chamber, and CORM-3 was added before O_2 exhaustion (c. 100 μM O_2; Fig. 1). On anoxia (maximum $CO:O_2$ ratio), the chamber was opened, allowing inward diffusion of air. Under these "open" conditions, the respiration rate is given as follows (13,14):

$$\nu_r = K(T_G - T_L) - dT_L/dt, \tag{1}$$

where ν_r is the respiration rate; K is a rate constant that is dependent on reaction volume, surface area, temperature, and others; T_G is the concentration of O_2 in the buffer when equilibrated with the gas phase; and T_L is the concentration of O_2 in the liquid sample at time t. Thus, at a constant rate of O_2 entry from the atmosphere, governed by the stirrer and liquid/air interface, inhibition or stimulation of respiration is indicated by an increase or decrease, respectively, in the measured O_2 tension.

Unexpectedly, addition of CORM-3 (100 μM final concentration) in the closed phase of the measurement (Fig. 1A, shaded portion) did not inhibit, but instead stimulated respiration by 36.8% (mean value of 34.7%, SEM 6.46%, four determinations in two biological repeats). After the chamber was opened, stimulation was still observed, here as a depression of the electrode trace (Fig. 1A, curved solid line) when compared with the no-CORM-control (dashed line). However, ~ 20 min after CORM-3 addition, inhibition of respiration was observed as the electrode trace increased above the steady-state level of the control. Thus, prolonged respiration measurements in the open system reveal an initial phase of respiratory stimulation, followed by inhibition.

As the CORM-3 concentration was increased to 250 μM (Fig. 1B) then 500 μM (Fig. 1C), the initial stimulation in the closed system increased slightly (up to 49.8% stimulation, SEM 3.53%), and inhibition occurred progressively earlier after CORM-3 addition.
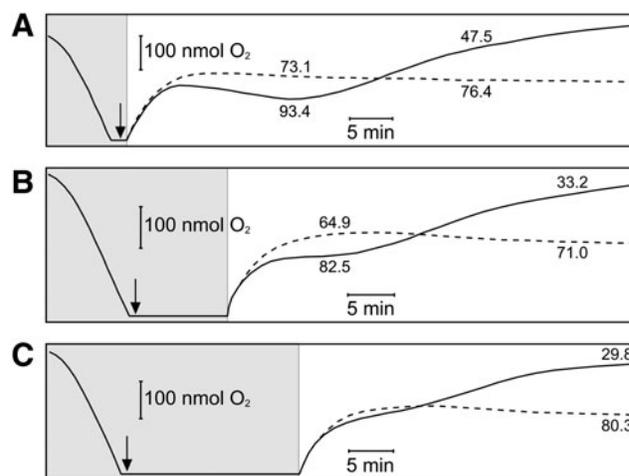
CORM-3 inhibition of bacterial respiration is enhanced by prior anoxia

Maximal inhibition of respiration is expected when the $CO:O_2$ ratio is increased, as CO is a competitive inhibitor of O_2 binding (28). We, therefore, modified the method to allow increased anoxic contact between the CO-RM and cells. In the absence of CORM-3, opening the chamber after brief anoxia (Fig. 2A, dashed line) results in a steady-state O_2 tension, as constant respiratory O_2 consumption is balanced by inward O_2 diffusion. However, when 100 μM CORM-3 was added at anoxia and the chamber opened immediately (Fig. 2A, solid line), respiration was initially stimulated (O_2 trace below the control level), then inhibited (O_2 trace above the control level). Increasing the period during which cells were incubated with CORM-3 from 0 min (Fig. 2A) to 10 min (Fig. 2B) or 20 min
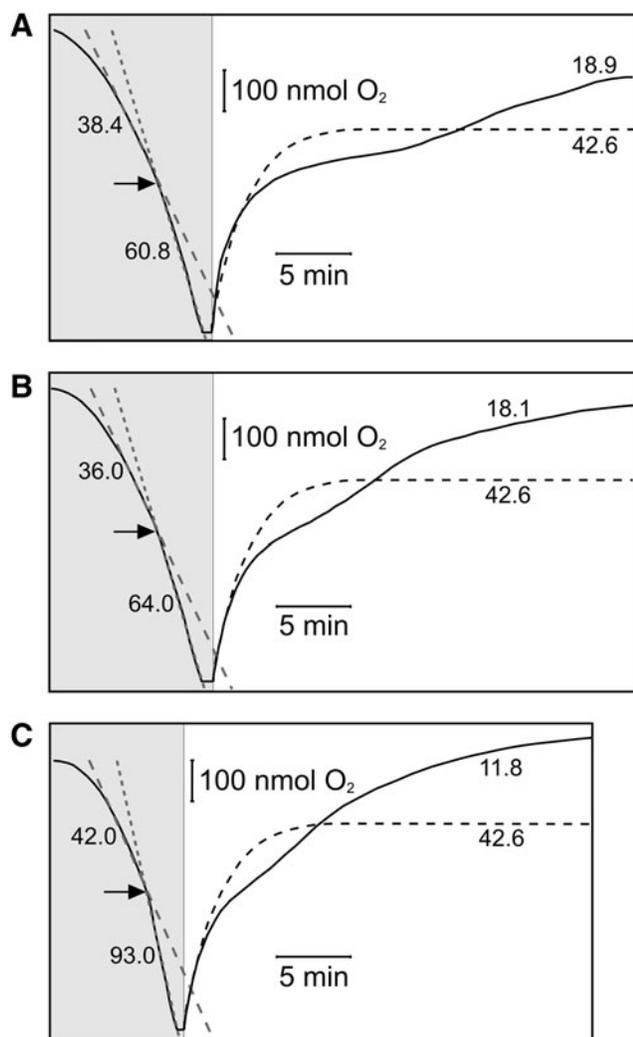
FIG. 1. Ru(CO)₃Cl(glycinate) (CORM-3) both stimulates and inhibits bacterial respiration in a concentration-dependent manner. O_2 utilization in a suspension of *E. coli* K-12 cells is represented as O_2 tension *versus* time. Bacteria were suspended in $50\,mM$ Tris buffer (pH 7.5), and respiration was stimulated by addition of $5\,mM$ glycerol. Shaded and unshaded sections indicate respiration traces recorded from the closed and open chamber, respectively. CORM-3 was added to a respiring suspension of *E. coli* at 50% air saturation (*arrow*) in the closed chamber. Dashed (before CORM-3 addition) and dotted (after CORM-3 addition) lines show extrapolated traces that highlight the change in gradient after the addition of compound. Rates of respiration (v_r: nmol·min⁻¹) are shown for each trace. The effects of $100\,\mu M$ **(A)**, $250\,\mu M$ **(B)**, and $500\,\mu M$ **(C)** CORM-3 on bacterial respiration are shown ($1.16\,mg$ cell protein). The control (nothing added) is shown as a dashed line. Traces are representative of ≥2 biological replicates with a maximum of three technical repeats per experiment.

FIG. 2. Inhibition of bacterial respiration is more potent after anoxic cell incubation with CORM-3. O_2 utilization in a suspension of *E. coli* K-12 cells is represented as O_2 tension *versus* time. The experimental design is as for Figure 1, except that, after complete consumption of O_2, nothing (control, dashed line) or $100\,\mu M$ CORM-3 (*arrow*, solid line) were added to the chamber and the lid was removed **(A)** immediately ($1.17\,mg$ cell protein), **(B)** after 10 min ($0.8\,mg$ cell protein), or **(C)** after 20 min ($0.8\,mg$ cell protein). Rates of respiration (v_r: nmol·min⁻¹) are shown for each trace. Traces are representative of three biological replicates.

marked phase of respiratory stimulation. The sequence of stimulation then inhibition, only the latter being anticipated from CO biochemistry, is not measurable in conventional short-term O_2 measurements.

To test the possibility that the phase of respiratory inhibition is accompanied by diversion of electrons to O_2 *via* non-oxidase routes, thus generating superoxide and peroxide [as in *Campylobacter jejuni* (59)], we added catalase during the inhibitory phase of an experiment which was similar to that shown in Figure 2A. No perturbation of the O_2 trace was observed (Supplementary Fig. S1; Supplementary Data are available online at www.liebertpub.com/ars), indicating a lack of significant hydrogen peroxide accumulation.

CORM-3-mediated "uncoupling" of respiration?

CORM-3 ($1–20\,\mu M$) "uncouples" mitochondrial respiration (22,50), deduced from the stimulation of respiration in State 2 [*i.e.*, the respiration that occurs on addition of substrate to mitochondria, but limited by lack of adenosine diphosphate (ADP) (41)]. CORM-3 also decreased mitochondrial membrane potential ($\Delta\Psi$). Both changes were gradual and slight compared with the instantaneous effects of only $1\,\mu M$ (or lower) carbonyl cyanide 4-(trifluoromethoxy)phenylhydrazone (FCCP) (41). Such compounds, generally referred to as "uncouplers," are better described as protonophores, catalyzing the net electrical uniport of H^+ and thus increasing the H^+ conductance of the membrane (41). However, the possible protonophore activity of CORM-3 was not directly tested (22,50).

Bacterial membranes are not known to possess the uncoupling proteins or adenine nucleotide transporters implicated in the modest "uncoupling" of mitochondria by

(Fig. 2C) before re-admitting O_2 progressively increased the degree of subsequent respiratory inhibition. Thus, when air was admitted immediately after CORM-3 addition, the mean inhibition was $41.4\%\pm3.58\%$; after 10 min, this rose to $53.7\%\pm1.46\%$ and, at 20 min, the inhibition was $61.2\%\pm2.63\%$. These increases in inhibition were accompanied by a less

CORM-3 (22); so, we sought direct evidence by measuring H^+ translocation using Mitchell's oxidant pulse technique (39). Here, a bacterial (or mitochondrial) lightly buffered suspension becomes anoxic by substrate oxidation. Respiration is re-initiated by injecting a known amount of O_2, and H^+ efflux (driven by H^+ pumps or vectorial chemistry) is recorded with a micro-pH electrode. Protonophores such as FCCP and carbonyl cyanide m-chlorophenylhydrazone (CCCP) collapse the measured H^+ extrusion.

Figure 3A shows H^+ pulses from *E. coli* cells in a medium containing K^+ plus valinomycin (a K^+-specific ionophore) and SCN^- (a permeant anion) to increase the rate and extent of H^+ pumping by neutralizing the thermodynamic back-pressure of the $\Delta\Psi$. Successive additions of air-saturated 150 mM potassium chloride (KCl) elicited acidification of the bulk medium due to respiration-driven H^+ translocation. H^+/O ratios, calculated after calibration with anoxic hydrochloric acid (HCl), were ~ 3 (mean 2.65 ± 0.11), that is, within the range of values reported for *E. coli* cells (33,48). Treatment of cells with the protonophore CCCP (35), which acts similar to FCCP, before O_2 additions dramatically reduced the H^+ pulses due to rapid H^+ exchange across the bacterial membrane (*i.e.*, true "uncoupling," Fig. 3B).

In contrast, previous treatment with CORM-3, followed by pH readjustment to compensate for loss of a H^+ from the CO-RM on addition to buffer, resulted in only a modest concentration-dependent reduction in the H^+/O ratio. CORM-3 at 20 μM (Fig. 3C) or 100 μM (Fig. 3D) attenuated only marginally the H^+/O ratios (mean $H^+/O = 2.51 \pm 0.06$, $H^+/O = 2.56 \pm 0.07$, respectively). Inactive CORM-3 [iCORM-3, *i.e.*, CORM-3 that was allowed to lose CO and then flushed with N_2 to displace CO from solution (8,22)] was without effect (Supplementary Fig. S2). In addition to measuring H^+/O ratios, we measured the rate of H^+ backflow after the O_2 pulse in the absence and presence of 20 μM CORM-3 and iCORM-3. In both cases, the $t_{1/2}$, measured from semi-log plots of pH changes were not significantly lowered by CORM-3 (1.45 min for CORM-3 and 1.66 min for corresponding control pulses; for iCORM-3 1.47 min and corresponding control pulses 1.57 min) (Supplementary Fig. S3).

Addition of 10 μM CCCP to an open O_2 electrode elicited the same downward deflection of the aerobic steady state (*i.e.*, stimulation of respiration; Fig. 3E) as that seen with 100 μM CORM-3 (cf. Fig. 2A). Cell viability was unaffected over 60 min by CCCP. Thus, CCCP, but not CORM-3, is a protonophore in *E. coli* cells, stimulating respiration rates and collapsing respiration-driven H^+ translocation.

Membrane potential is not dissipated by CORM-3

The transmembrane pH gradient (ΔpH) and $\Delta\psi$ together constitute the protonmotive force (pmf). Protonophores shuttle H^+ across the lipid bilayer, effectively short-circuiting the transmembrane H^+ gradient and transiently stimulating respiration when electron transport is coupled to H^+ translocation (41). Protonophores dissipate both the ΔpH and $\Delta\psi$ components of the pmf. To determine whether CORM-3 affects the $\Delta\psi$ of respiring *E. coli*, CORM-3 (100 μM) was pre-incubated with cells (for 0–20 min) and the $\Delta\psi$ determined (Fig. 4). Under the experimental conditions used here, the external pH is buffered at pH 7.5, and, therefore, the total pmf is predominantly $\Delta\psi$. The $\Delta\psi$ of untreated cells was
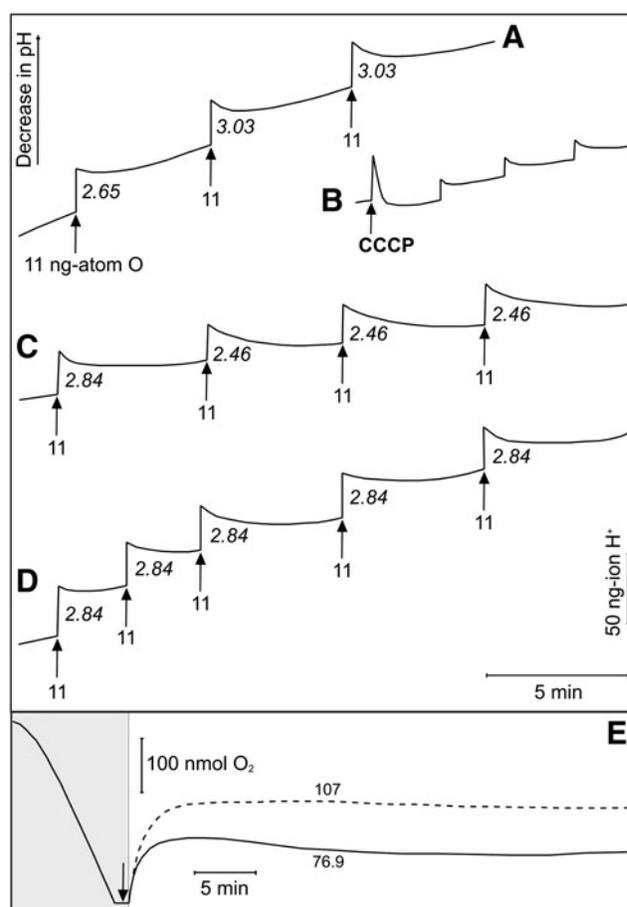
FIG. 3. CORM-3 is not a true "uncoupler" or protonophore. Bacteria were added to lightly buffered solution in a closed chamber, followed by immediate addition of valinomycin (22 μM) and stimulation of respiration (1 mM glycerol). The experiment commenced after complete consumption of O_2. *Arrows* show additions of air-saturated 150 mM potassium chloride (30°C, 11 ng-atom O), each of which is immediately followed by H^+ efflux (acidification, upward deflection). The H^+/O ratio for each pulse is shown. **(A)** Representative control pulses [no carbon monoxide–releasing molecule (CO-RM) added] (5.43 mg cell protein), mean $H^+/O = 2.65 \pm 0.11$, 9 determinations; **(B)** pulses after addition of 4 nmol (1.6 μM) carbonyl cyanide m-chlorophenylhydrazone (CCCP) (5.43 mg cell protein); **(C)** 20 μM CORM-3 (5.64 mg cell protein), mean $H^+/O = 2.51 \pm 0.06$, 13 determinations (1.2% lower than control); and **(D)** 100 μM CORM-3 (5.43 mg cell protein), $H^+/O = 2.56 \pm 0.07$, 15 determinations (3.4% lower than control). Data are representative of three biological replicates, with ≥ 3 technical repeats per experiment. *Panel* **(E)** shows the effect of 10 μM CCCP added to *E. coli* suspended in 50 mM Tris (pH 7.5) (0.91 mg cell protein) after complete consumption of O_2 in an electrode chamber. The chamber was opened immediately after addition of compound (*arrow*), and the effect of 10 μM CCCP (solid line) was compared with the control (nothing added, dashed line). Rates of respiration (v_r: nmol·min^{-1}) are shown for each trace. Traces are representative of the given number of determinations from three biological replicates.
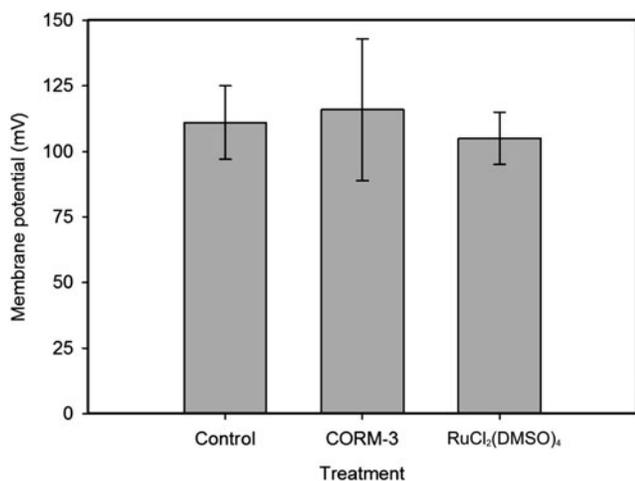
FIG. 4. Effects of CORM-3 and RuCl₂(DMSO)₄ on transmembrane potential of *E. coli* cell suspensions. CORM-3 and $RuCl_2(DMSO)_4$ (100 μM each) were preincubated aerobically with glycerol-energized cells for 20 min before measurement of the $\Delta\psi$. Technical replicates were performed on all samples, and the standard error of the mean across a number of experiments is shown.

111 ± 15 mV (Fig. 4). Cells treated with CORM-3 had a $\Delta\psi$ of 116 ± 27 mV (range 95–143 mV); thus, the CO-RM has a mild stimulatory effect on the $\Delta\psi$, but did not dissipate the $\Delta\psi$ even with 20 min of incubation (Fig. 4). Cells treated with the control molecule $RuCl_2(DMSO)_4$ (100 μM) had a $\Delta\psi$ of 105 ± 10 mV. These data demonstrate directly that CORM-3 does not dissipate the $\Delta\psi$ of respiring cells.

CORM-3 does not directly stimulate oxidase activity

Having demonstrated that the stimulatory effect of CORM-3 cannot be attributed to protonophore activity, we investigated other potential mechanisms. Interestingly, low doses of CO (10 μM) transiently stimulate cytochrome *c* oxidase activity in mitochondria; however, the overall effects on organelle or cell respiration were not reported (49). To eliminate transmembrane ion fluxes from consideration here, respiration of isolated membranes, not bacterial cells, was measured. When bacteria are disrupted by harsh physical methods such as ultrasonication, membranes are fragmented and form "leaky" vesicles of mixed orientation that are unsuitable for transport measurements (41,46). We measured respiration in such vesicles using both open and closed electrode systems (Fig. 5). In the conventional closed system, addition of high concentrations of CORM-3 (400 μM) were required to inhibit initial rates of respiration by >50% (Fig. 5A). In the open system, which allowed more protracted measurements and CO-RM addition at low (35 μM) poised O_2 levels (Fig. 5B), respiration was reduced to one-third of the control rate by CORM-3 (100 μM). Importantly, in neither experiment was stimulation of respiration observed, suggesting that this phenomenon is associated with ion fluxes rather than catalytic function of the quinol oxidases.

### K^+ and Na^+, not H^+, transport is facilitated by CORM-3

Membrane channels other than those for H^+ are modified by CO and CO-RMs in eukaryotic cells. The effect may be
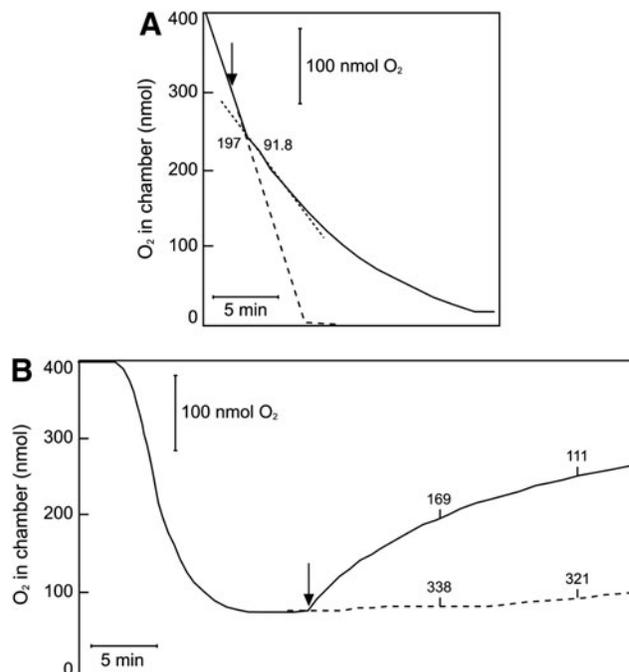
FIG. 5. CORM-3 does not directly stimulate respiratory oxidase activity. *E. coli* membrane particles resuspended in Tris-HCl buffer were added to an O_2 electrode chamber to a final concentration of 170 $\mu g/ml$. Respiration was stimulated by the addition of nicotinamide adenine dinucleotide at final concentrations of 6.25 mM **(A)** or 12.5 mM **(B)**. *Panel* **(A)** shows O_2 consumption in a closed chamber. CORM-3 (400 μM, solid line) was added at ~75% air saturation (155 μM O_2) (*arrow*). *Panel* **(B)** shows O_2 consumption in an open chamber. The O_2 concentration of the suspension was allowed to equilibrate at ~18% air saturation (35 μM O_2), and CORM-3 (100 μM, solid line) was added 2 min after a steady-state had been reached (*arrow*). O_2 consumption in the absence of the compound (dashed line) is also shown for both experiments. Rates of respiration [v_r: nmol·min^{-1}·(mg protein)$^{-1}$] in **(A)** at 2 min and **(B)** at 10 and 20 min after the addition of CORM-3, or at the equivalent time points in the control experiment, are shown. For both types of experiments the traces are typical of two biological repeats, with three technical replicates per experiment.

indirect, caused by an interaction between critical Cys residues with reactive O_2 species generated from CO inhibition of mitochondrial respiration (56) or by a direct interaction between CO and channel proteins (21). CORM-2 is an allosteric inhibitor of voltage-gated K^+ channels, reducing the voltage dependence of the opening transition (24). We, therefore, tested whether CORM-3 promotes cation transport using osmotic swelling of spheroplasts (18). Iso-osmotic sucrose (0.5 M) provides support to detergent- and osmotically-sensitive spheroplasts, as shown by constant light-scattering properties (18). For swelling to occur, both cation and anion should enter to prevent charge imbalance; water follows, causing the spheroplasts to swell.

Spheroplast behavior in iso-osmotic solutions of NO_3^- salts is shown in Figure 6A; the NO_3^- anion freely permeates the spheroplast membrane (18). Iso-osmotic potassium nitrate (KNO_3) (0.25 M) provided osmotic support until spheroplasts
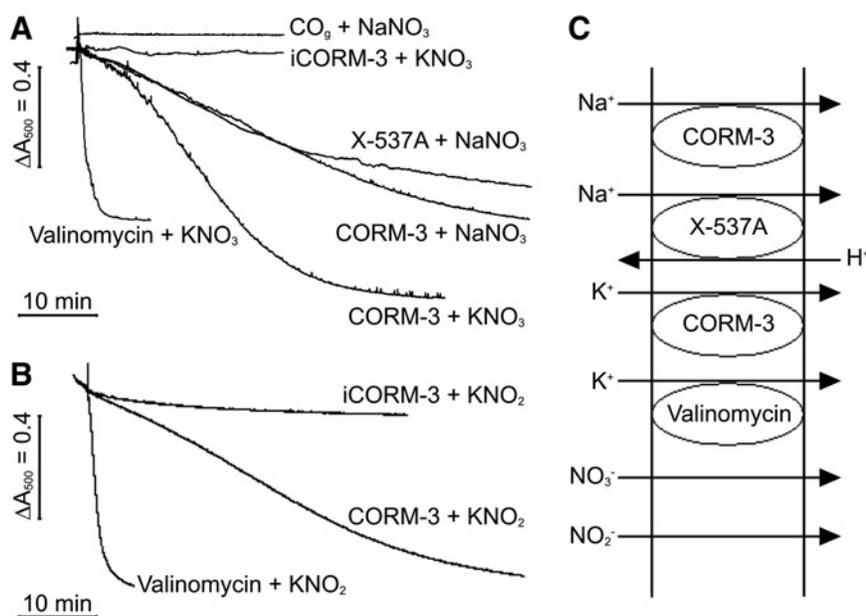
FIG. 6. CORM-3 promotes K^+ and Na^+ fluxes across the bacterial membrane. Osmotic behavior of spheroplast suspensions ($OD_{500} \sim 0.5$) in 0.25 M potassium nitrate (KNO_3) and sodium nitrate ($NaNO_3$) **(A)**, or potassium nitrite (KNO_2) **(B)** was monitored *via* light scattering at 500 nm after addition of 100 μM CORM-3, 100 μM iCORM-3, valinomycin, or X-537A (each 1 $\mu g/\mu l$). **(C)** CORM-3 facilitates movement of K^+ and Na^+ ions from the extracellular space (*left* of membrane) to the cytoplasm (*right*) through the cytoplasmic membrane (vertical lines). Since the NO_3^- and NO_2^- anions are freely permeable, the pathway provided by CORM-3 or an established ionophore allows swelling. Traces are representative of ≥ 2 biological repeats, with three technical replicates per experiment.

were treated with valinomycin (Fig. 6A). This effect was mimicked, although more slowly, by 100 μM CORM-3, showing it to have ionophore-like properties (Fig. 6A), but iCORM-3 did not promote spheroplast swelling (Fig. 6A). When spheroplasts were suspended in 0.25 M sodium nitrate ($NaNO_3$), further addition of the Na^+ ionophore X-537A (lasalocid) or of CORM-3 was required for swelling (Fig. 6A) despite the facile permeation of the NO_3^- anion. X-537A promotes transport of a number of monovalent and divalent cations, including Na^+, in an electroneutral exchange with H^+ (26,41). A solution of CO gas (final concentration 100 μM) did not promote swelling (Fig. 6A), indicating that CO alone does not act as an ionophore for Na^+ ions.

Spheroplast behavior in iso-osmotic solutions of NO_2^- salts is shown in Figure 6B; the NO_2^- anion also freely permeates spheroplasts (18). Thus, in iso-osmotic 0.25 M potassium nitrite (KNO_2), swelling was again promoted by either valinomycin or CORM-3 (Fig. 6B), as both nitrous acid (HNO_2) and the NO_2^- anion can cross the membrane (18).

The K^+, Na^+, H^+, NO_3^-, and NO_2^- movements responsible are shown in Figure 6C along with the activities of established ionophores. Based on these data, CORM-3 simulates the effects of K^+ and Na^+ ionophores.

### Ru compounds that do not release CO, or CO gas, do not inhibit respiration

The commonly used CO-RMs have properties other than CO release that may interfere in biological processes. In particular, CORM-3 is a Ru carbonyl, Ru being a metal ion with redox chemistry that does not occur naturally in biology. Further, CO release may also be accompanied by loss of glycinate, chloride, and other unknown processes and interactions. To demonstrate that the stimulatory and inhibitory effects of CORM-3 on bacterial respiration are due specifically to CO release, we used three Ru-containing control molecules. $RuCl_2(DMSO)_4$ is a control for CORM-2, a precursor in CORM-3 synthesis (8), in which the CO groups are replaced by DMSO (53). When used at 100 μM (Fig. 7A, solid line),

neither stimulation nor inhibition of respiration was observed (compare with Fig. 2A). The same result (Fig. 7B, solid line) was obtained with iCORM-3. Both these compounds are imperfect controls: $RuCl_2(DMSO)_4$ lacks the glycinate group of CORM-3, and iCORM has not been exposed to biological species that induce release of more CO than can be achieved by gassing. We, therefore, devised a new control (myoglobin-inactivated CORM-3, miCORM-3) where CO is removed by two treatments with myoglobin [dissociation constant, $CO = 27 \mu M^{-1}$ (58)]. This preparation, when tested with ferrous myoglobin, gave no detectable CO release (Fig. 7C, inset) and did not elicit the same response as CORM-3 (Fig. 7C, solid line compared with gray dotted line). We conclude that CO release is necessary for the perturbing effects of CORM-3 on bacterial respiration.

We previously reported (11) that solutions of CO gas were without effect on *E. coli*, when used at concentrations equimolar with inhibitory levels of CORM-3. Figure 7D–F show that, irrespective of the period (up to 20 min) during which 100 μM CO and cells were incubated anoxically to maximize the $CO:O_2$ ratio, CO neither stimulated nor inhibited respiration (solid lines). In mitochondria, a modest increase in State 2 respiration is reported, but only at grossly nonphysiological (960 μM) CO concentrations (22).

CORM-3 as an antimicrobial agent: viability loss is coincident with effects on respiration

Earlier, we (15) showed that inhibition of respiration preceded loss of *P. aeruginosa* viability, but did not observe bacterial respiratory stimulation. In the present study, we sampled from an open O_2 electrode chamber to simultaneously measure O_2 uptake and bacterial viability. On adding CORM-3 to this low-density culture, an initial phase of respiratory stimulation (downward deflection of the O_2 trace) followed by inhibition (upward deflection) was observed (Fig. 8A) as before (Fig. 2). Within 10 min of adding 100 μM CORM-3 to a culture, cell viability was reduced by 90% (Fig. 8B) and, within 20 min, the number of viable cells was below the limits
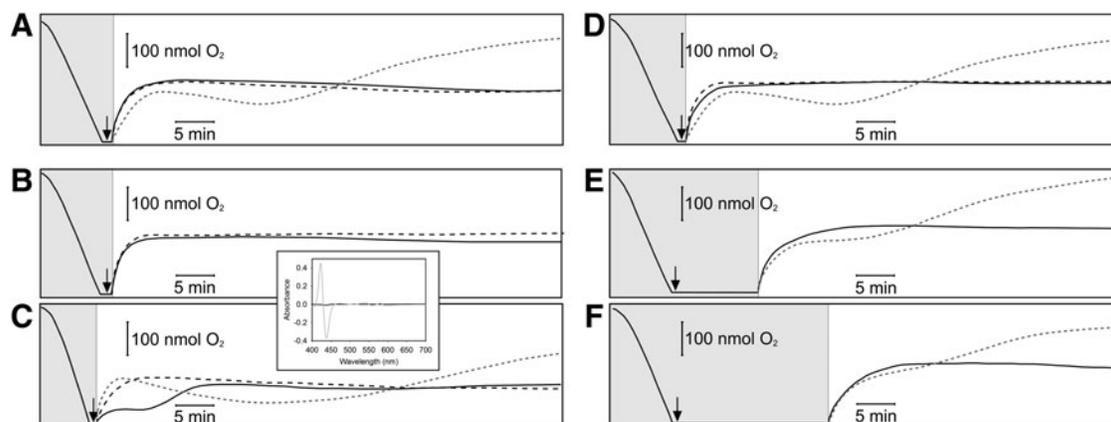
FIG. 7. Ru-containing control molecules and CO have minimal effects on bacterial respiration. O_2 utilization in a suspension of *E. coli* K-12 cells is represented as O_2 tension *versus* time. Bacteria were suspended in 50 mM Tris buffer (pH 7.5), and respiration was stimulated by addition of 5 mM glycerol. Shaded and unshaded sections indicate respiration traces recorded from the closed and open chamber, respectively. CORM-3 control compounds, or CO saturated solution, were added after complete O_2 consumption (*arrows*). The chamber was opened immediately after injection of control compounds (solid lines): **(A)** 100 μM RuCl$_2$(DMSO)$_4$ (0.53 mg cell protein); the trace for 100 μM CORM-3 in Figure 2A has been superimposed for ease of reference (gray dotted line), **(B)** 100 μM inactive CORM-3 (iCORM-3) (0.67 mg cell protein), and **(C)** 50 μM myoglobin-inactivated CORM-3 (miCORM-3) (0.85 mg cell protein); the trace for 50 μM CORM-3 is shown for ease of reference (gray dotted line). Inactivity of miCORM-3 (black line) is shown *inset* by a lack of CO release to ferrous myoglobin compared with CORM-3 (gray line). In each *panel*, black dashed lines represent control traces (nothing added). The effect of 100 μM CO saturated solution (solid lines) after different periods of anoxia is shown in comparison with control (nothing added, black dashed line): **(D)** The chamber was opened immediately after addition (0.73 mg cell protein), **(E)** 10 min post-addition (0.73 mg cell protein), or **(F)** 20 min post-addition (0.72 mg cell protein). Control traces overlaid the traces recorded after exposure to CO in *panels* **B** and **C**. In each case, traces shown for 100 μM CORM-3 in Figure 2 have been superimposed for reference (gray dotted line). Traces are representative of ≥2 biological replicates.

of detection ($< 9 \times 10^6$ cells). These parallel measurements of O_2 tension and viability show that loss of viability began and was largely completed during the phase of stimulation, before respiratory inhibition.

### Reversal by photolysis of respiratory inhibition protects cells from CORM-3-induced killing

The photoreversibility of CO inhibition of respiration was exploited in the classical photochemical action spectrum approach to identifying terminal oxidases (4). Although CO-RMs inhibit respiration, and the CO binds to terminal oxidases (11,15), it has not been demonstrated formally that respiratory inhibition *in vivo* is due to CO reactivity with oxidases. To test this hypothesis, we treated membranes in a glass chamber with CORM-3 and measured respiration rates during light–dark cycles (Fig. 9A). Addition of 300 μM CORM-3 inhibited respiration completely when the O_2 in the chamber was reduced to $\sim 45 \mu M$ using N_2-saturated buffer (Fig. 9A). Exposure to actinic light reversed this effect, and repeated light–dark cycles confirmed that CORM-3 inhibition was reversible by white light, thus identifying heme oxidases(s) as primary respiratory target(s).

We reasoned that, since cells are killed by CORM-3 during respiratory perturbations (Fig. 8A, B) and since inhibition of respiration is light-reversible (Fig. 9A), then cell viability may be protected from CORM-3 under illumination. This hypothesis is supported by Figure 9B; 30 μM CORM-3 elicited a drop in cell survival after exposure to actinic light, such that, at 60 min, $\sim 30\%$ of the initial viable counts remained. However, the viability loss was dramatically exacerbated in the dark; 95% of the population was killed in 60 min (Fig. 9B). We

could not determine whether cells "recover" when cultures are switched from dark to light because the effects of CO-RMs are not bacteriostatic, but bactericidal as shown in Figure 8 and elsewhere (11,43).

CORM-3 is an inhibitor of respiration in pathogenic bacteria and yeast

CORM-3 (25–100 μM) inhibited respiration not only of *E. coli* but also of *P. aeruginosa* (Supplementary Fig. S4A), in which inhibition of growth has previously been reported (15), and *Salmonella enterica* serovar Typhimurium (Supplementary Fig. S4B). For *P. aeruginosa*, the inhibition of respiration elicited by 25, 50, and 100 μM CORM-3 was typically 23.7%, 61.7%, and 74.7% ~ 30 min after CORM-3 addition. In *S.* Typhimurium, the inhibition of respiration elicited by 50 μM CORM-3 was typically 74.8% 30 min after addition. Respiratory stimulation was not observed in these species. Control experiments employing one or more iCORM-3 compounds [RuCl$_2$(DMSO)$_4$, iCORM-3, and miCORM-3] showed that only CORM-3 was effective. In *S.* Typhimurium, for example, 50 μM miCORM-3 was not a respiratory inhibitor (Supplementary Fig. S4B). Although CORM-3 also inhibited respiration of *Candida albicans*, higher concentrations were required (250–500 μM; Supplementary Fig. S4C) than for bacteria (Supplementary Fig S4A, B). These concentrations typically inhibited respiration by 13.4% and 39.0%, respectively. At lower concentrations (50–100 μM), opening the electrode chamber led to a continuous decline in dissolved O_2 due to uninhibited respiration, which was identical to the control (*i.e.*, no CO-RMs added). Again, 250 and 500 μM iCORM-3 were ineffective.
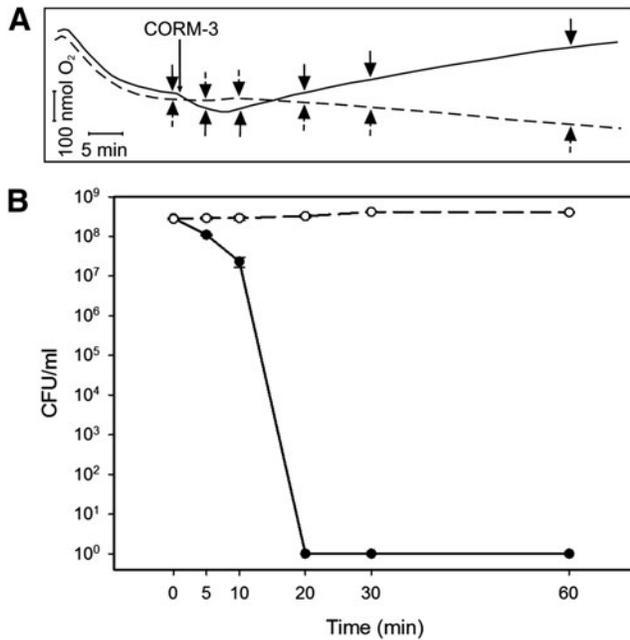
FIG. 8.   **CORM-3 elicits cell death at the onset of respiratory effects.** Cells were suspended in defined medium in an O_2 electrode chamber at a concentration that was sufficient to result in a steady state at c. 25% air saturation. O_2 utilization is represented as O_2 tension *versus* time. *E. coli* viability over the course of the experiment was determined from parallel chamber samples. **(A)** Effect of 100 μM CORM-3 (solid line) on O_2 uptake in comparison with control (nothing added, dashed line, 0.31 mg cell protein). *Arrows* indicate points at which samples were taken to assay viability; solid *arrows* correspond to the CORM-3-treated suspension; and dashed *arrows* correspond to the control suspension. **(B)** Effect of 100 μM CORM-3 (solid line) on viability in comparison with control (nothing added, dashed line). Sampling time points are aligned with *arrows* that indicate removal of suspension (*panel* **A**) to show the respiratory trace and cell counts in parallel. Traces are representative of three biological replicates.

Discussion

Utilizing CO gas as an antimicrobial therapeutic (6) is thwarted by CO toxicity and the systemic delivery methods necessary (40). CO-RMs allow localized CO delivery, but the fate of administered CO-RMs is poorly understood. Although CO-RMs release CO inside bacteria (11,43), we do not understand the biochemical basis of CO-RM action. In the case of CORM-2 and ALF062, a contributing factor is the generation of oxidative stress (61). Here, we demonstrate unequivocally that CORM-3 is a potent inhibitor of microbial respiration, and rapid loss of bacterial viability correlates temporally with the interference of respiratory metabolism (Fig. 8).

CO is widely used as a probe for hemes in biology and for oxidase identification and studies of ligand binding/exchange [*e.g.*, (19)]. We previously demonstrated oxidase–CO adducts in CO-RM-treated cells (11,15) and here show that such complexes are photolabile at ambient temperatures with moderate intensities of visible light; photolysis reverses respiratory inhibition, alleviating the loss of cell viability (Fig. 9). To our knowledge, this is the first evidence that the bio-

logical consequences of CO release from a CO-RM can be reversed by light, although CO-RMs that release CO on irradiation have been described [reviewed in (54)]. These findings have important implications for future therapeutic applications of CO-RMs in the light.

Several lines of evidence suggest that the mode of action is more complex than the release of CO at concentrations equal to the administered CO-RMs. First, unlike other inhibitors of bacterial oxidases, for example, cyanide (23,64), inhibition by CORM-3 in whole cells is slow and not readily observed in a conventional, closed O_2 electrode. This is presumably because of the need for the CO-RMs to penetrate the cell and interact with cellular species [*e.g.*, (38)] that displace CO. Respiratory inhibition is accelerated by preincubating cells with CO-RMs under anoxic conditions (Fig. 2), thus maximizing the $CO:O_2$ ratio and binding of CO to target hemes, as reported for hypoxic mitochondria (10).

A further complexity is the stimulation of respiratory rates that precedes inhibition (Figs. 1 and 2). This can indicate not only protonophore activity in bacteria as in the case of CCCP (Fig. 3B) or nisin (12) but also the action of any compound that catalyzes electrogenic ion movement. As here, Iacono *et al.* (22) showed in mitochondria that the effect of CORM-3 was unlike that of protonophores. First, much higher CO-RM concentrations (around 2–50 μM) were needed than for FCCP (0.02–1 μM) to observe stimulation of State 2 respiration, which was more marked and instantaneous with the latter compound (2.4-fold stimulation with 20 μM CORM-3 *vs.* 6.3-fold with 1 μM FCCP). Second, mitochondrial $\Delta\psi$ was minimally affected by CORM-3 compared with FCCP. The effect of 0.02 μM FCCP was similar to that of 20 μM CORM-3, whereas 1 μM FCCP collapsed the potential instantaneously. No direct measurements of H^+ fluxes accompanying respiratory stimulation, the hallmarks of a classical protonophore, were reported (22), although the "recoupler" 6-ketocholestanol did not affect mitochondrial stimulation by CORM-3 (22). Further, in models of renal function and sepsis, low CORM-3 concentrations increased the respiratory control index, a measure of the tightness of coupling (31,51). In the present bacterial case, there was no collapse of the pmf as expected (Figs. 3 and 4; Supplementary Fig. S3). CO gas slightly enhances terminal oxidase activity in mitochondria (1), but not in *E. coli* (Fig. 7D–F). We suggest that the term "uncoupling," to describe CO-RM-promoted respiration, is inappropriate, as it implies a dissociation (*i.e.*, uncoupling) between the processes of respiratory electron transfer and adenosine triphosphate (ATP) synthesis (41), as in the "uncoupled" (*unc*) mutants of *E. coli* with defects in the F_oF_1 ATP synthase (16). We conclude that CORM-3 stimulates respiration not by acting as a protonophore but rather by its transient effects on ion transport and pmf.

Despite similarities between the effects of CORM-3 on mitochondria (22) and bacteria, there are important differences. First, the concept of States 2 (ADP-limited) and 3 (ADP-stimulated) (5) to describe the effects of ADP availability on respiration tightly coupled to ATP synthesis is not generally applied to bacteria. Respiratory stimulation in bacteria by ADP, to which bacteria are impermeable, is not easily demonstrated, although the effects of protonophores can sometimes be observed as a stimulation of respiration (45). ADP/ATP exchange cannot be measured in fragmented bacterial membrane vesicles, and intact bacteria are not susceptible to
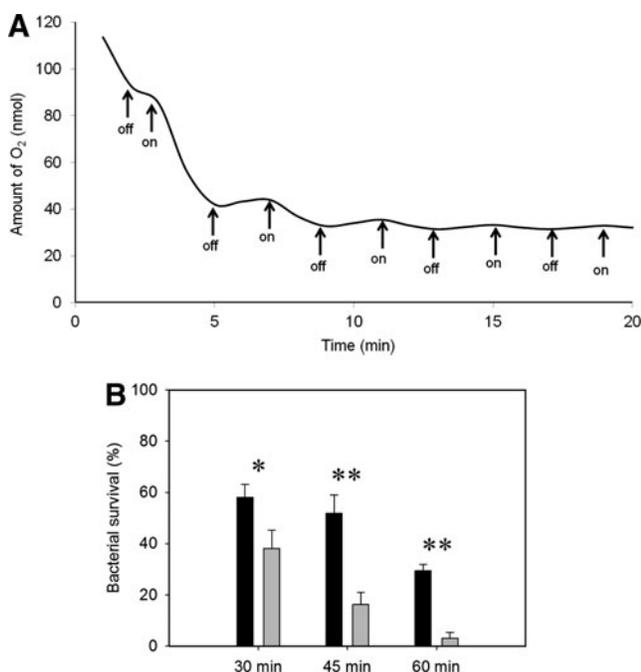
FIG. 9. Light abrogates the toxic effects of CORM-3 by photolyzing heme-CO bonds. (A) O_2 consumption of *E. coli* membrane particles (0.17 mg membrane protein) treated with 300 μM CORM-3. White light focused on the glass chamber was switched on and off at 2-min intervals (as indicated by the *arrows*). **(B)** Viable counts were performed on cultures of *E. coli* treated with 30 μM CORM-3 grown either in light (black bars) or dark (gray bars) conditions. The mean bacterial survival of five technical repeats at 30, 45, and 60 min compared with the viability before the addition of CORM-3 is shown and is representative of three biological replicates. Asterisks indicate statistically significant decreases in viability of cultures grown in the dark compared with cultures grown in the light, as measured using the Student's *t*-test (*$p < 0.001$; **$p = 0$).

oligomycin used before (22) to block ATP synthase activity. Further, 5-hydroxydecanoate, an inhibitor of mitochondrial ATP-dependent K^+ channels, did not reduce CO-RM-elicited respiratory stimulation, whereas, in the present study, CORM-3 was an effective K^+ and Na^+ ionophore (Fig. 6). The basis of the promoting effect on K^+ transport is currently unclear; *E. coli* possesses several systems for transport of K^+, the major intracellular cation, which is maintained at 0.1–0.5 M. The most attractive candidate may be Kch (30), the first prokaryotic K^+ channel to be identified with clear homology to those eukaryotic voltage-activated K^+ channels that CORM-2 modulates (24). A recent report (49) suggests that CO prevents, not promotes, mitochondrial permeabilization, thereby preventing swelling, but the effect appears unlinked to K^+ permeability.

A probable explanation of the greater effectiveness of CO-RMs, compared with CO gas, is that the intracellular concentrations of CO achieved by CO-RM administration are significantly higher than for CO gas, despite the facile diffusion of CO through membranes. Based on Ru analysis, the intracellular level of CORM-3 is >200 μM after adding only 30 μM to growing cultures (11). The preferential release of CO inside cells is consistent with recent data showing that CO

release rates from CORM-3 are greatly enhanced by sulfite, but not by a reaction of CORM-3 with globins without such a ligand (38). In the present work, corroborating evidence for the requirement of an intracellular or other complex biological milieu is provided by Figure 7D–F that fails to show effects of CO. Further, CO gas did not promote cation transport (Fig. 6A).

We now propose a "Trojan Horse" mechanism for the antimicrobial actions of CO-RMs to explain the potent effects on respiration that cannot be mimicked by CO gas (Fig. 10). In brief, a CO-RM may lose its CO permanently in the extracellular milieu through, for example, the presence of a species to capture the CO or a change in the CO-RM after CO loss. Alternatively, the CO-RM is transported into the cell and concentrated (11) carrying its CO cargo (Trojan Horse effect), and CO dissociation is promoted by a reaction with intracellular ligands that include sulfite (38). Thus, CO is immediately accessible at relatively high concentrations to membrane-bound heme targets, to which it binds. Respiration is inhibited in a light-reversible manner, and viability is drastically reduced.

Nonheme targets for CO may explain, in part, the diverse effects of CO and CO-RMs (3,34,40). There are many examples of nonheme Fe(II) carbonyls, and ligands from amino acids (S in Cys and N in His) may be targets in voltage-gated (Slo1 BK) channels that are important in vasodilation (21) or
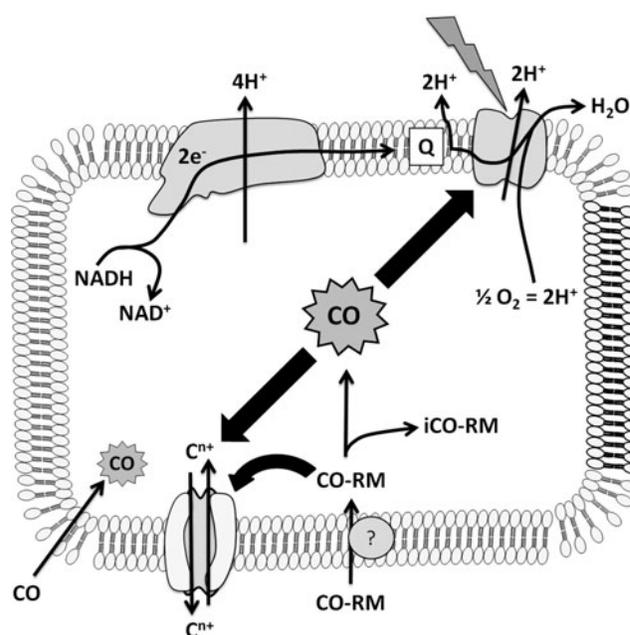
FIG. 10. Trojan Horse hypothesis. It is postulated that CO-RMs carry their CO "toxic cargo" into the cell interior by unknown mechanisms. Intracellular accumulation of CO-RMs and subsequent release of CO leads to CO reaching concentrations (*center* of cell) that exceed those which can be attained by passive diffusion of CO gas from the cell exterior (*bottom left*). The major targets of CORM-3 identified in this work are respiratory electron transfer to O_2, catalyzed by terminal quinol oxidases, and cation transport. Inhibition of respiration and growth inhibition is reversed by white light at ambient temperatures (*top right*). The scheme excludes the bacterial outer membrane and periplasm and the representation of the respiratory chain, terminating in a single oxidase, is greatly simplified.

in bacterial ion channels (Fig. 6). Other nonheme targets are likely: In *Chlamydomonas* hydrogenase, CO binds to an Fe-Fe center (60), and CO also binds to binuclear copper sites as in tyrosinase (29) and hemocyanins (17,62). Identifying modes of action is critical if CO and CO-RMs are to be used therapeutically.

Materials and Methods

Microbial strains and growth conditions

E. coli K-12 MG1655 (RKP5416) (2), *P. aeruginosa* PAO1 (RKP5417), *S. enterica* serovar Typhimurium (RKP4901), and a clinical isolate of *C. albicans* (CA3153 302, kind gift from Professor P. Sudbery, The University of Sheffield) were used. *E. coli* and *S.* Typhimurium were grown in defined medium with glycerol (54 mM) (11). *P. aeruginosa* was grown in minimal M9 medium with glucose (11.1 mM) as a carbon source (15). *C. albicans* was grown in defined medium containing D-glucose (111 mM) and yeast nitrogen base (6.8 g/L). Bacteria were grown aerobically in 20–30 ml medium in 250 ml flasks fitted with side arms for measurements of optical density with a Klett meter (red filter) during shaking at 200 rpm and 37°C.

CORM-3 and control treatments

Aqueous stock solutions of CORM-3 (25) and RuCl$_2$(DM-SO)$_4$ (the latter compound supplied by Dr. Tony Johnson, Chemistry Department, The University of Sheffield) at 10 or 100 mM were made fresh each day. iCORM-3 was prepared (8,22) by dissolving CORM-3 in phosphate-buffered saline (PBS), allowing CO liberation to the atmosphere for 48 h at room temperature, and bubbling with O$_2$-free N$_2$ (BOC; GU2 5XY) periodically throughout the incubation to ensure dissociation and loss of CO. miCORM-3 was prepared by treating CORM-3 twice with a twofold excess of ferrous myoglobin, prepared by adding sodium dithionite solution (2.2 mM final concentration in 0.1 M potassium phosphate, pH 7) to 1 mM metmyoglobin. Carbonmonoxy myoglobin was separated from the required inactivated CORM-3 residue by centrifugation in a Vivaspin 20 concentrator (Sartorius Stedim Biotech) with a molecular weight cutoff of 5 kDa. CORM-3 or inactivated CO-RMs were added directly to cells suspended in medium or 50 mM Tris (pH 7.5) in an O$_2$ electrode chamber. CO was added as a solution saturated with the gas by bubbling from a cylinder (BOC) at room temperature. CO release from CORM-3 and control molecules to ferrous myoglobin was assayed (8,38) in a dual-wavelength scanning spectrophotometer (27). Data were plotted as CO reduced *minus* reduced spectra (63).

O$_2$ consumption

Cultures were harvested at midexponential phase, washed, and resuspended in medium or 50 mM Tris buffer (pH 7.5). Cells were suspended in a stirred Perspex chamber fitted with a Clark-type polarographic O$_2$ electrode (OXY041A; Rank Brothers Ltd.; CB25 9DA) at 37°C (20). Data were recorded on a chart reader (REC112; Amersham Pharmacia Biotech) or a Lab-Trax-4/16 recorder and Data-Trax™ software (World Precision Instruments, Inc.). Protein concentrations were measured using a modified Lowry procedure (37). Respiration was stimulated by the addition of glycerol or nicotinamide adenine dinucleotide (NADH). An "open" O$_2$ electrode

system was used in most experiments, in which a stirred sample is open to the atmosphere, allowing continuous O$_2$ diffusion from the vortex surface into the sample; prolonged measurements can be made without O$_2$ depletion (14). To correlate O$_2$ consumption and bacterial viability, cells were added to the chamber at a low concentration that would result in a steady-state level of c. 25% air saturation. Samples were taken and diluted in PBS followed by plating drops (diluted 10^{-5}–10^{-8}) on nutrient agar for viability counts.

Photosensitivity of respiratory inhibition and loss of viability elicited by CORM-3

Bacteria were grown in 1 L Luria broth (LB) medium in 2 L baffled flasks at 37°C with shaking at 250 rpm until late exponential phase. Membranes were prepared (46) and incubated in a glass chamber (RC350 respiration cell; Strathkelvin Instruments Limited; ML1 5RX) with 1.95 ml N$_2$-saturated buffer (50 mM Tris-HCl, 2 mM magnesium chloride, and 1 mM ethylene glycol tetraacetic acid; 37°C), then treated with 300 μM ethylene CORM-3. A microcathode O$_2$ electrode (SI130; Strathkelvin Instruments Limited) located in the chamber lid was connected to an O$_2$ meter (Model 781) and then to a Lab-Trax-4/16 recorder and Data-Trax software as described earlier. Respiration was stimulated with 12.5 mM NADH. A 150 W projector bulb was focused on the wall of the glass chamber using a convex lens, giving an intensity of 175,000 lux at the vessel surface.

To make parallel measurements of respiration rate and bacterial viability, bacteria were grown to midexponential phase (50 Klett units) in defined medium. Samples (2 ml) were transferred to two parallel glass respiration cells, as described earlier, and stirred at 37°C; one was foil-wrapped, and an actinic light beam was focused on the other as described earlier. Samples were taken immediately before addition of 30 μM CORM-3 and at intervals thereafter for viability counts.

Respiration-driven H$^+$ translocation across the bacterial membrane

The apparatus was based on (32,33) incorporating a sealed, stirred Perspex chamber fitted with a Clark-type polarographic O$_2$ electrode (OXY040A; Rank Brothers Ltd; CB25 9DA) at 30°C. The lid of the chamber was modified to support a semimicro calomel combined pH electrode (pHC4000; MeterLab; Radiometer Analytical). The signal from the pH electrode was taken to a pH/ion meter (PHM240; MeterLab; Radiometer Analytical) and then to a potentiometric recorder.

E. coli was grown aerobically at 37°C and 200 rpm in defined medium supplemented with 0.1% casamino acids to midexponential phase. Cells were starved by shaking for 2 h in medium lacking carbon sources, harvested by centrifugation at 4°C, washed twice, and resuspended in cold 150 mM KCl. An aliquot was added to 2.5 ml lightly buffered medium (150 mM KCl, 50 mM potassium cyanide, and 1.5 mM glycylglycine; pH 7; 30°C) in the chamber. Valinomycin (Sigma-Aldrich; 22 μM final concentration, added as a methanolic stock solution) was added immediately after, followed by 1 mM glycerol to stimulate respiration. The experiment commenced after consumption of O$_2$. Additions of an anoxic solution of 5 mM HCl were used to calibrate the apparatus (25–75 ng-ion H$^+$). Pulses of air-saturated 150 mM KCl (30°C) (25 μl, 11 ng-atom O) were added to promote respiration-

driven H$^+$ translocation and medium acidification. CCCP (Sigma-Aldrich; 1.6 μM final concentration) was used as protonophore. H$^+$/O ratios were calculated from deflections caused by the acid and O$_2$ pulses.

[^{3}H]methyltriphenylphosphonium iodide accumulation

The $\Delta\psi$ of washed cell suspensions optical density (OD$_{600}$ ~ 1.2) in 50 mM Tris buffer (pH 7.5) was determined by measuring the accumulation of [^{3}H]methyltriphenylphosphonium iodide ([^{3}H]TPMP$^+$, 30–60 Ci/mmol; 10 nM final concentration, NEN™; Life Science Products, Inc.) using filtration assays (0.45-μm cellulose-acetate filters; Sartorius Stedim Biotech) (55) after incubation at 37°C. Filters were washed twice with 2 ml of 100 mM lithium chloride and dried for 60 min at 40°C. Filters were resuspended in 2 ml of scintillation liquid, and counts per minute were determined using an LKB Wallac 1214 Rackbeta liquid scintillation counter. The $\Delta\psi$ was calculated from the Nernst equation ($\Delta\psi = 62 \times \log$ [TPMP]$_{in}$/[TPMP]$_{out}$), and an intracellular volume of $2.8 \pm 0.5\,\mu$l per mg of protein was used (57).

Spheroplasts and osmotic swelling measurements

Cells were grown in 400 ml LB, harvested at mid-exponential phase and spheroplasts were prepared (36). Cells were washed once in 10 mM Tris-HCl (pH 7.4) and resuspended in 20% (w/v) sucrose containing 33 mM Tris-HCl (pH 8) to an OD$_{600}$ of c. 0.8. The suspension was stirred gently at 4°C with additions of 0.01 ml of 0.1 M ethylenediaminetetraacetic acid (pH 8) and 1 μl of lysozyme (5 mg/ml) (per ml suspension). Osmotic fragility was checked by 10-fold dilutions into water and measuring decreasing turbidity at 500 nm. When spheroplast formation was complete (no further reduction in OD$_{500}$), they were harvested at 4°C, washed once, and resuspended gently in the same Tris/sucrose buffer using a loose-fitting hand homogenizer. Osmotic swelling was studied (18) by following the change in turbidity at 500 nm, using a Cary 50 spectrophotometer (Varian), following dilution of spheroplast samples in iso-osmotic 0.25 M solutions of KNO$_3$, KNO$_2$, or NaNO$_3$. Valinomycin and X-537A (Sigma-Aldrich; acetonitrile solution) were used at final concentrations of 1 μg/μl.

Acknowledgments

Author Disclosure Statement

B.E. Mann declares a financial interest in Alfama. All other authors declare that no competing financial interests exist.

References

1. Almeida AS, Queiroga CSF, Sousa MFQ, Alves PM, and Vieira HLA. Carbon monoxide modulates apoptosis by reinforcing oxidative metabolism in astrocytes. Role of Bcl-2. *J Biol Chem* 287: 10761–10770, 2012.
2. Blattner FR, Plunkett G, Bloch CA, Perna NT, Burland V, Riley M, ColladoVides J, Glasner JD, Rode CK, Mayhew GF, Gregor J, Davis NW, Kirkpatrick HA, Goeden MA, Rose DJ, Mau B, and Shao Y. The complete genome sequence of *Escherichia coli* K-12. *Science* 277: 1453–1462, 1997.
3. Boczkowski J, Poderoso JJ, and Motterlini R. CO-metal interaction: vital signaling from a lethal gas. *Trends Biochem Sci* 31: 614–621, 2006.
4. Castor LN, and Chance B. Photochemical action spectra of carbon monoxide-inhibited respiration. *J Biol Chem* 217: 453–465, 1955.
5. Chance B, and Williams GR. The respiratory chain and oxidative phosphorylation. *Adv Enzmol* XVll: 65–134, 1956.
6. Chin BY, and Otterbein LE. Carbon monoxide is a poison... to microbes! CO as a bactericidal molecule. *Curr Opin Pharmacol* 9: 490–500, 2009.
7. Chung SW, Liu X, Macias AA, Baron RM, and Perrella MA. Heme oxygenase-1-derived carbon monoxide enhances the host defense response to microbial sepsis in mice. *J Clin Invest* 118: 239–247, 2008.
8. Clark JE, Naughton P, Shurey S, Green CJ, Johnson TR, Mann BE, Foresti R, and Motterlini R. Cardioprotective actions by a water-soluble carbon monoxide-releasing molecule. *Circ Res* 93: e2–8, 2003.
9. Cooper CE, and Brown GC. The inhibition of mitochondrial cytochrome oxidase by the gases carbon monoxide, nitric oxide, hydrogen cyanide and hydrogen sulfide: chemical mechanism and physiological significance. *J Bioenerg Biomembr* 40: 533–539, 2008.
10. D'Amico G, Lam F, Hagen T, and Moncada S. Inhibition of cellular respiration by endogenously produced carbon monoxide. *J Cell Sci* 119: 2291–2298, 2006.
11. Davidge KS, Sanguinetti G, Yee CH, Cox AG, McLeod CW, Monk CE, Mann BE, Motterlini R, and Poole RK. Carbon monoxide-releasing antibacterial molecules target respiration and global transcriptional regulators. *J Biol Chem* 284: 4516–4524, 2009.
12. de Melo AMSC, Cook GM, Miles RJ, and Poole RK. Nisin stimulates oxygen consumption by *Staphylococcus aureus* and *Escherichia coli*. *Appl Environ Microbiol* 62: 1831–1834, 1996.
13. Degn H, Lilleor M, and Iversen JJL. The occurrence of a stepwise-decreasing respiration rate during oxidative assimilation of different substrates by resting *Klebsiella aerogenes* in a system open to oxygen. *Biochem J* 136: 1097–1104, 1973.
14. Degn H, Lundsgaard JS, Petersen LC, and Ormicki A. Polarographic measurement of steady state kinetics of oxygen uptake by biochemical samples. *Methods Biochem Anal* 26: 47–77, 2006.
15. Desmard M, Davidge KS, Bouvet O, Morin D, Roux D, Foresti R, Ricard JD, Denamur E, Poole RK, Montravers P, Motterlini R, and Boczkowski J. A carbon monoxide-releasing molecule (CORM-3) exerts bactericidal activity against *Pseudomonas aeruginosa* and improves survival in an animal model of bacteraemia. *FASEB J* 23: 1023–1031, 2009.
16. Fimmel AL, Jans DA, Hatch L, James LB, Gibson F, and Cox GB. The F$_1$F$_0$-ATPase of *Escherichia coli*. The substitution of alanine by threonine at position 25 in the c-subunit affects function but not assembly. *Biochim Biophys Acta* 808: 252–258, 1985.
17. Finazzi-Agro A, Zolla L, Flamigni L, Kuiper HA, and Brunori M. Spectroscopy of (carbon monoxy)hemocyanins. Phosphorescence of the binuclear carbonylated copper centers. *Biochemistry* 21: 415–418, 1982.
18. Garland PB, Downie JA, and Haddock BA. Proton translocation and the respiratory nitrate reductase of *Escherichia coli*. *Biochem J* 152: 547–559, 1975.

19. Gibson QH, Greenwood C, Wharton DC, and Palmer G. Reaction of cytochrome oxidase with cytochrome *c*. *J Biol Chem* 240: 888–894, 1965.

20. Gilberthorpe NJ, and Poole RK. Nitric oxide homeostasis in *Salmonella typhimurium*—roles of respiratory nitrate reductase and flavohemoglobin. *J Biol Chem* 283: 11146–11154, 2008.

21. Hou SW, Xu R, Heinemann SH, and Hoshi T. The RCK1 high-affinity Ca2+ sensor confers carbon monoxide sensitivity to Slo1 BK channels. *Proc Natl Acad Sci U S A* 105: 4039–4043, 2008.

22. Iacono L, Boczkowski J, Zini R, Salouage I, Berdaux A, Motterlini R, and Morin D. A carbon monoxide-releasing molecule (CORM-3) uncouples mitochondrial respiration and modulates the production of reactive oxygen species. *Free Radic Biol Med* 50: 1556–1564, 2011.

23. Jackson RJ, Elvers KT, Lee LJ, Gidley MD, Wainwright LM, Lightfoot J, Park SF, and Poole RK. Oxygen reactivity of both respiratory oxidases in *Campylobacter jejuni*: the *cydAB* genes encode a cyanide-resistant, low-affinity oxidase that is not of the cytochrome *bd* type. *J Bacteriol* 189: 1604–1615, 2007.

24. Jara-Oseguera A, Ishida IG, Rangel-Yescas GE, Espinosa-Jalapa N, Perez-Guzman JA, Elias-Vinas D, Le Lagadec R, Rosenbaum T, and Islas LD. Uncoupling charge movement from channel opening in voltage-gated potassium channels by ruthenium complexes. *J Biol Chem* 286: 16414–16425, 2011.

25. Johnson TR, Mann BE, Teasdale IP, Adams H, Foresti R, Green CJ, and Motterlini R. Metal carbonyls as pharmaceuticals? [Ru(CO)$_3$Cl(glycinate)], a CO-releasing molecule with an extensive aqueous solution chemistry. *Dalton Trans* 1500–1508, 2007.

26. Jundt H, Porzig H, Reuter H, and Stucki JW. The effect of substances releasing intracellular calcium ions on sodium-dependent calcium efflux from guinea-pig auricles. *J Physiol* 246: 229–253, 1975.

27. Kalnenieks U, Galinina N, Bringer-Meyer S, and Poole RK. Membrane D-lactate oxidase in *Zymomonas mobilis*: evidence for a branched respiratory chain. *FEMS Microbiol Lett* 168: 91–97, 1998.

28. Keilin D. *The History of Cell Respiration and Cytochrome*. Cambridge: Cambridge University Press, 1966, pp. 416.

29. Kuiper HA, Lerch K, Brunori M, and Finazzi Agro A. Luminescence of the copper-carbon monoxide complex of *Neurospora tyrosinase*. *FEBS Lett* 111: 232–234, 1980.

30. Kuo MM, Saimi Y, and Kung C. Gain-of-function mutations indicate that *Escherichia coli* Kch forms a functional K$^+$ conduit *in vivo*. *EMBO J* 22: 4049–4058, 2003.

31. Lancel S, Hassoun SM, Favory R, Decoster B, Motterlini R, and Neviere R. Carbon monoxide rescues mice from lethal sepsis by supporting mitochondrial energetic metabolism and activating mitochondrial biogenesis. *J Pharmacol Exp Ther* 329: 641–648, 2009.

32. Lawford HG, and Garland PB. Proton translocation coupled to quinol oxidation in ox heart mitochondria. *Biochem J* 136: 711–720, 1973.

33. Lawford HG, and Haddock BA. Respiration-driven proton translocation in *Escherichia coli*. *Biochem J* 136: 217–220, 1973.

34. Li L, and Moore PK. An overview of the biological significance of endogenous gases: new roles for old molecules. *Biochem Soc Trans* 35: 1138–1141, 2007.

35. Lou PH, Hansen BS, Olsen PH, Tullin S, Murphy MP, and Brand MD. Mitochondrial uncouplers with an extraordinary dynamic range. *Biochem J* 407: 129–140, 2007.

36. Malamy MH, and Horecker BL. Release of alkaline phosphatase from cells of *Escherichia coli* upon lysozyme spheroplast formation. *Biochemistry* 3: 1889–1893, 1964.

37. Markwell MAK, Haas SM, Bieber LL, and Tolbert NE. A modification of the Lowry procedure to simplify protein determination in membrane and lipoprotein samples. *Anal Biochem* 87: 206–210, 1978.

38. McLean S, Mann B, and Poole RK. Sulfite species enhance CO release from CO-releasing molecules: implications for the deoxymyoglobin assay of activity. *Anal Biochem* 247: 36–40, 2012.

39. Mitchell P, and Moyle J. Respiration-driven proton translocation in rat liver mitochondria. *Biochem J* 105: 1147–1162, 1967.

40. Motterlini R, and Otterbein LE. The therapeutic potential of carbon monoxide. *Nat Rev Drug Discov* 9: 728–743, 2010.

41. Nicholls DG, and Ferguson SJ. *Bioenergetics 3*. London: Academic Press, 2002.

42. Nobre LS, Al-Shahrour F, Dopazo J, and Saraiva LM. Exploring the antimicrobial action of a carbon monoxide-releasing compound through whole-genome transcription profiling of *Escherichia coli*. *Microbiology* 155: 813–824, 2009.

43. Nobre LS, Seixas JD, Romao CC, and Saraiva LM. Antimicrobial action of carbon monoxide-releasing compounds. *Antimicrob Agents Chemother* 51: 4303–4307, 2007.

44. Otterbein LE, May A, and Chin BY. Carbon monoxide increases macrophage bacterial clearance through toll-like receptor (TLR)4 expression. *Cell Mol Biol* 51: 433–440, 2005.

45. Poole RK. The influence of growth substrate and capacity for oxidative phosphorylation on respiratory oscillations in synchronous cultures of *Escherichia coli* K12. *J Gen Microbiol* 99: 369–377, 1977.

46. Poole RK. The isolation of membranes from bacteria. In: Graham JM, and Higgins JA, eds. *Biomembrane Protocols. 1. Isolation and Analysis*. Totowa, New Jersey: Humana Press, 1993, pp. 109–122.

47. Poole RK, and Cook GM. Redundancy of aerobic respiratory chains in bacteria? Routes, reasons and regulation. *Adv Microb Physiol* 43: 165–224, 2000.

48. Poole RK, and Haddock BA. Effects of sulphate-limited growth in continuous culture on the electron-transport chain and energy conservation in *Escherichia coli* K12. *Biochem J* 152: 537–546, 1975.

49. Queiroga CSF, Almeida AS, Alves PM, Brenner C, and Vieira HLA. Carbon monoxide prevents hepatic mitochondrial membrane permeabilization. *BMC Cell Biol* 12: 10, 2011.

50. Sandouka A, Balogun E, Foresti R, Mann BE, Johnson TR, Tayem Y, Green CJ, Fuller B, and Motterlini R. Carbon monoxide-releasing molecules (CO-RMs) modulate respiration in isolated mitochondria. *Cell Mol Biol* 51: 425–432, 2005.

51. Sandouka A, Fuller BJ, Mann BE, Green CJ, Foresti R, and Motterlini R. Treatment with carbon monoxide-releasing molecules (CO-RMs) during cold storage improves renal function at reperfusion. *Kidney Int* 69: 239–247, 2006.

52. Sanguinetti G, Lawrence ND, and Rattray M. Probabilistic inference of transcription factor concentrations and gene-specific regulatory activities. *Bioinformatics* 22: 2775–2781, 2006.

53. Sawle P, Foresti R, Mann BE, Johnson TR, Green CJ, and Motterlini R. Carbon monoxide-releasing molecules (CO-RMs) attenuate the inflammatory response elicited by lipopolysaccharide in RAW264.7 murine macrophages. *Br J Pharmacol* 145: 800–810, 2005.

54. Schatzschneider U. PhotoCORMs: light-triggered release of carbon monoxide from the coordination sphere of transition

metal complexes for biological applications. *Inorg Chim Acta* 374: 19–23, 2011.

55. Schuldiner S, and Kaback HR. Membrane potential and active transport in membrane vesicles from *Escherichia coli*. *Biochemistry* 14: 5451–5461, 1975.

56. Scragg JL, Dallas ML, Wilkinson JA, Varadi G, and Peers C. Carbon monoxide inhibits L-type Ca2 + channels via redox modulation of key cysteine residues by mitochondrial reactive oxygen species. *J Biol Chem* 283: 24412–24419, 2008.

57. Shepherd M, Sanguinetti G, Cook GM, and Poole RK. Compensations for diminished terminal oxidase activity in *Escherichia coli* cytochrome bd-II-mediated respiration and glutamate metabolism. *J Biol Chem* 285: 18464–18472, 2010.

58. Smerdon SJ, Krzywda S, Brzozowski AM, Davies GJ, Wilkinson AJ, Brancaccio A, Cutruzzola F, Allocatelli CT, Brunori M, Li T, *et al.* Interactions among residues CD3, E7, E10, and E11 in myoglobins: attempts to simulate the ligand-binding properties of *Aplysia* myoglobin. *Biochemistry* 34: 8715–8725, 1995.

59. Smith H, Mann BE, Motterlini R, and Poole RK. The carbon monoxide-releasing molecule, CORM-3 (Ru(CO)$_3$Cl(Glycinate)), targets respiration and oxidases in *Campylobacter jejuni*, generating hydrogen peroxide. *IUBMB Life* 63: 363–371, 2011.

60. Stripp ST, Goldet G, Brandmayr C, Sanganas O, Vincent KA, Haumann M, Armstrong FA, and Happe T. How oxygen attacks [FeFe] hydrogenases from photosynthetic organisms. *Proc Natl Acad Sci U S A* 106: 17331–17336, 2009.

61. Tavares AF, Teixeira M, Romao CC, Seixas JD, Nobre LS, and Saraiva LM. Reactive oxygen species mediate bactericidal killing elicited by carbon monoxide-releasing molecules. *J Biol Chem* 286: 26708–26717, 2011.

62. van der Deen H, and Hoving H. An infrared study of carbon monoxide complexes of hemocyanins. Evidence for the structure of the co-binding site from vibrational analysis. *Biophys Chem* 9: 169–179, 1979.

63. Wood PM. Bacterial proteins with CO-binding b- or c-type haem. Functions and absorption spectroscopy. *Biochim Biophys Acta* 768: 293–317, 1984.

64. Zlosnik JEA, Tavankar GR, Bundy JG, Mossialos D, O'Toole R, and Williams HD. Investigation of the physiological relationship between the cyanide-sensitive oxidase and cyanide production in *Pseudomonas aeruginosa*. *Microbiology* 152: 1407–1415, 2006.

Address correspondence to:
Prof. Robert K. Poole
Department of Molecular Biology and Biotechnology
The University of Sheffield
Sheffield S10 2TN
United Kingdom

E-mail: r.poole@sheffield.ac.uk

Abbreviations Used

$\Delta\psi$ = membrane potential
ADP = adenosine diphosphate
ALF062 = tetraethylammonium molybdenum pentacarbonyl bromide
ATP = adenosine triphosphate
CCCP = carbonyl cyanide-*m*-chlorophenylhydrazone
CO-RM = carbon monoxide-releasing molecule
CORM-2 = tricarbonyl dichlororuthenium (II) dimer
CORM-3 = Ru(CO)$_3$Cl(glycinate)
FCCP = trifluoromethoxyphenylhydrazone
HO = heme oxygenase
iCORM = CO-RM from which CO is removed by allowing CO to escape
LB = Luria broth
miCORM-3 = CORM-3 from which CO is removed by reaction with dithionite and myoglobin
NADH = nicotinamide adenine dinucleotide
ng-atom(s) O = g-atoms oxygen×10^{-9}, equal to nmol O$_2$ × 2
OD = optical density
PBS = phosphate-buffered saline
pmf = protonmotive force
TPMP$^+$ = methyltriphenylphosphonium iodide